

LYMPHOID NEOPLASIA

The double-hit signature identifies double-hit diffuse large B-cell lymphoma with genetic events cryptic to FISH

Laura K. Hilton,¹ Jeffrey Tang,¹ Susana Ben-Neriah,² Miguel Alcaide,¹ Aixiang Jiang,^{1,2} Bruno M. Grande,¹ Christopher K. Rushton,¹ Merrill Boyle,² Barbara Meissner,² David W. Scott,^{2,3,*} and Ryan D. Morin^{1,4,*}

¹Department of Molecular Biology and Biochemistry, Simon Fraser University, Burnaby, BC, Canada; ²BC Cancer Centre for Lymphoid Cancer, BC Cancer Research Centre, Vancouver, BC, Canada; ³Department of Medicine, University of British Columbia, Vancouver, BC, Canada; and ⁴Genome Sciences Center, British Columbia Cancer Agency, Vancouver, BC, Canada

KEY POINTS

- Gene expression identifies DHITsig⁺ DLBCL tumors with *BCL2* and *MYC* translocations detectable by whole-genome sequencing, but not by breakapart FISH.
- Additional genetic mechanisms of *MYC* dysregulation include focal *MYC* and *MIR17HG* copy-number gains and *PVT1* promoter deletions.

High-grade B-cell lymphomas with *MYC* and *BCL2* and/or *BCL6* rearrangements (HGBL-DH/THs) include a group of diffuse large B-cell lymphomas (DLBCLs) with inferior outcomes after standard chemoimmunotherapy. We recently described a gene expression signature that identifies 27% of germinal center B-cell DLBCLs (GCB-DLBCLs) as having a double-hit-like expression pattern (DHITsig) and inferior outcomes; however, only half of these cases have both *MYC* and *BCL2* translocations identifiable using standard breakapart fluorescence in situ hybridization (FISH). Here, 20 DHITsig⁺ GCB-DLBCLs apparently lacking *MYC* and/or *BCL2* rearrangements underwent whole-genome sequencing. This revealed 6 tumors with *MYC* or *BCL2* rearrangements that were cryptic to breakapart FISH. Copy-number analysis identified 3 tumors with *MYC* and 6 tumors with *MIR17HG* gains or amplifications, both of which may contribute to dysregulation of *MYC* and its downstream pathways. Focal deletions of the *PVT1* promoter were observed exclusively among DHITsig⁺ tumors lacking *MYC* translocations; this may also contribute to *MYC* overexpression. These results highlight that FISH fails to identify all HGBL-DH/THs, while revealing a range of other genetic mechanisms potentially underlying *MYC* dysregulation in DHITsig⁺ DLBCL, suggesting that gene expression profiling is more sensitive for identifying the biology underlying poor outcomes in GCB-DLBCL. (*Blood*. 2019;134(18):1528-1532)

Introduction

Diffuse large B-cell lymphomas (DLBCLs) are a genetically heterogeneous group of neoplasms with variable outcomes after standard chemoimmunotherapy (eg, R-CHOP [rituximab plus cyclophosphamide, doxorubicin, vincristine, and prednisone]). There is an ongoing interest in delineating subgroups within DLBCL that share targetable biology, with the potential for precision medicine to overcome biology currently associated with treatment failure. Among the subgroups with the worst outcomes, high-grade B-cell lymphomas with *MYC* and *BCL2* (and sometimes *BCL6*) rearrangements (HGBL-DH/TH-*BCL2*s) mostly belong to the germinal center B-cell (GCB) molecular subgroup (the subgroup generally considered to have favorable prognosis).^{1,2} We recently defined a gene expression signature that identifies nearly one-third of GCB-DLBCL tumors as having a double-hit-like gene expression pattern (DHITsig), with only half harboring rearrangements of both *MYC* and *BCL2* as determined by breakapart fluorescence in situ hybridization (FISH).³ In that cohort, the outcomes for the 20 non-HGBL-DH/TH-*BCL2* patients were comparable to those of patients with HGBL-DH/TH-*BCL2*.

In contrast to Burkitt lymphoma (BL), where the partner of *MYC* is universally an immunoglobulin gene, in approximately half of HGBL-DH/THs with DLBCL morphology, the partner is nonimmunoglobulin.⁴ For this reason, a breakapart FISH strategy is favored for detecting *MYC* rearrangements in DLBCL rather than *MYC/IGH* dual fusion. Breakapart FISH purportedly fails to detect 2% to 4% of *MYC* rearrangements when the false-negative cases are identified using an *MYC/IGH* dual-fusion approach.⁵⁻⁷ Recently, a BL tumor was described where the coding exons of *MYC* (8.6 kb) were inserted into the *IGH* locus, an event cryptic to both FISH approaches.⁸ This raises the possibility that a proportion of DLBCLs harbor *MYC* and/or *BCL2* rearrangements that are cryptic to FISH.

We hypothesized that genetic dysregulations of *MYC* and *BCL2* and their downstream signaling pathways are among the fundamental genetic events underlying the DHITsig in most, if not all, DHITsig⁺ DLBCL tumors. Using whole-genome sequencing (WGS) of 20 tumors lacking *MYC* and/or *BCL2* rearrangements by FISH, we identified 6 cases with rearrangements cryptic to

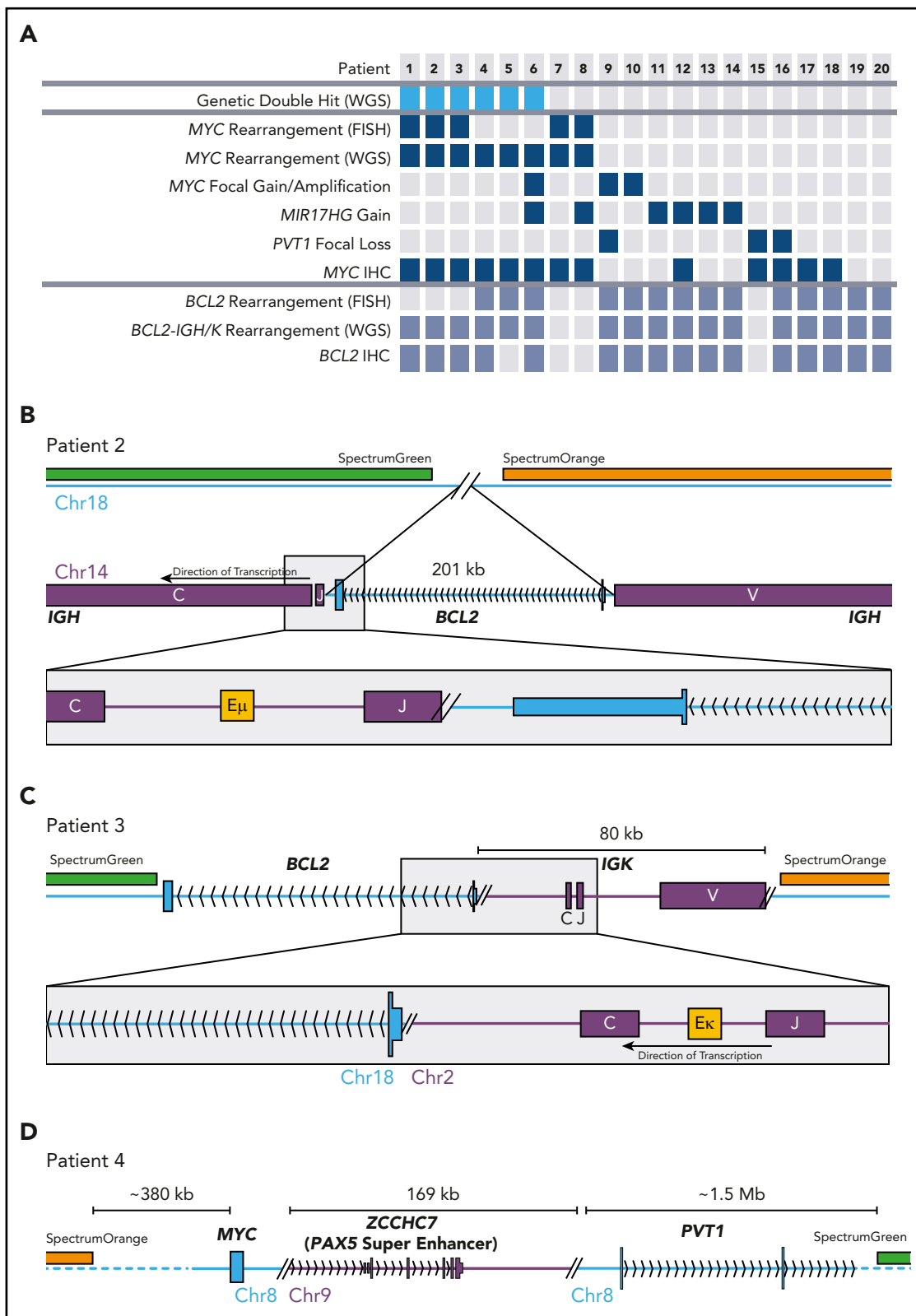


Figure 1. FISH-cryptic MYC and BCL2 rearrangements identified by WGS in DHITsig⁺ DLBCL tumors. (A) Diagram summarizing the occurrence of each genetic event identified in the 20 non-HGBL-DH/TH-BCL2DHITsig⁺ genomes. The thresholds for MYC and BCL2 immunohistochemistry (IHC) positivity were 40% and 50%, respectively. (B-C) Cryptic BCL2 translocations identified in tumors that were negative for BCL2 rearrangement by breakpart FISH. (D) A cryptic MYC rearrangement identified in a tumor that was negative for MYC rearrangement by breakpart FISH.

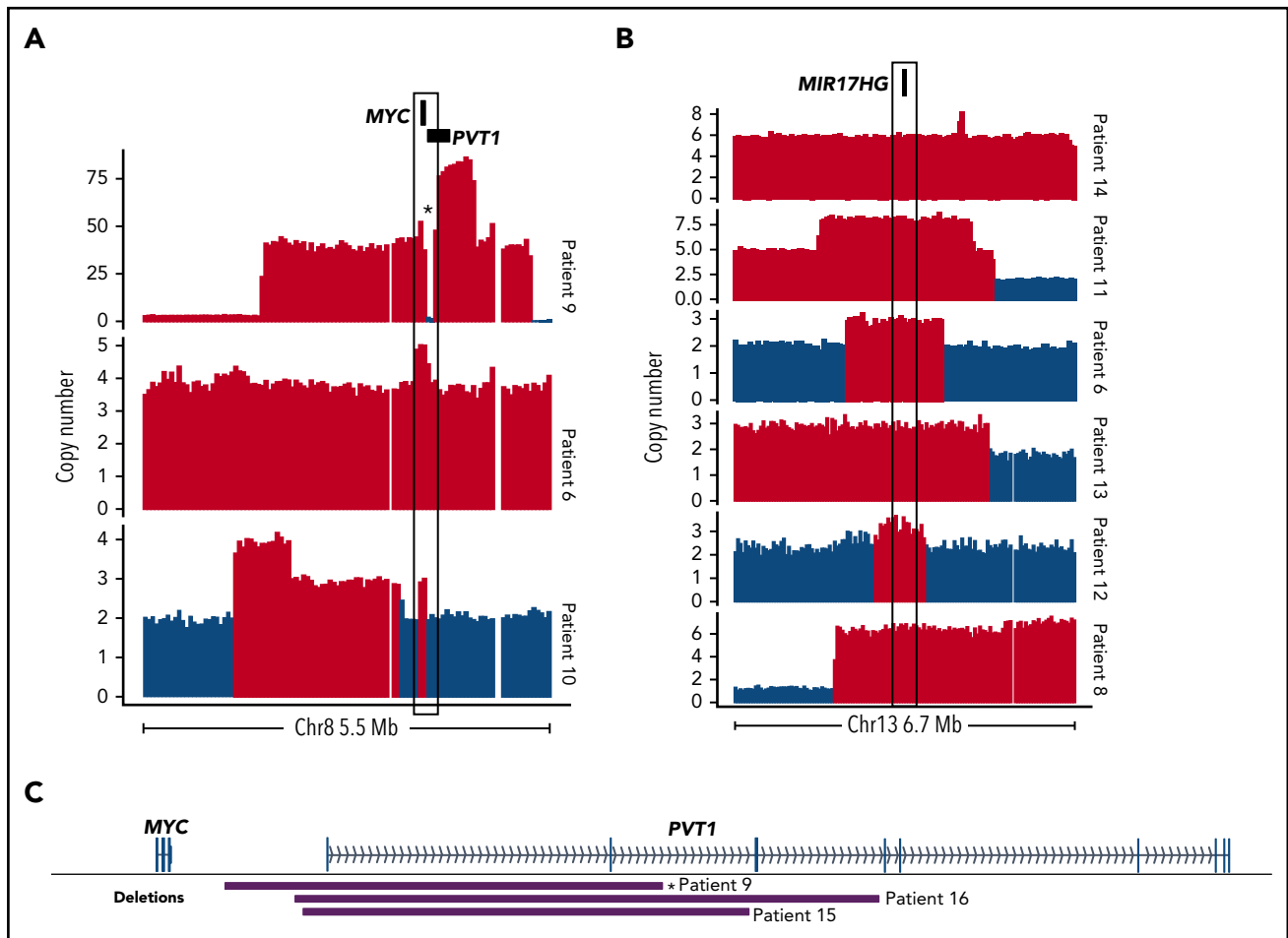


Figure 2. Somatic CNVs affecting *MYC*, *MIR17HG*, and *PVT1* identified by WGS among DHITsig⁺ DLBCL tumors. Focal copy-number gains of *MYC* (A) or *MIR17HG* (B) identified among DHITsig⁺ DLBCL tumors. Red bars indicate regions where Control-FREEC identified a significant increase in copy number ($P < .05$). Compared with 162 GCB tumors without a *MIR17HG* amplification as determined by single-nucleotide polymorphism (SNP) arrays, expression of *MIR17HG* was significantly elevated among these 6 cases with *MIR17HG* copy gains (log₂ fold change, 0.85; Wilcoxon $P = .032$). (C) The boundaries of focal *PVT1* transcription start site (TSS) deletions identified in DHITsig⁺ tumors. *Indicates the *PVT1* deletion identified in the double-minute chromosome.

breakapart FISH, along with other genetic mechanisms of dysregulation of *MYC* and downstream pathways.

Methods

DNA was extracted from the 20 fresh-frozen GCB DHITsig⁺ tumors lacking *MYC* and/or *BCL2* translocations (breakapart FISH) identified by Ennishi et al.³ Polymerase chain reaction-free libraries were constructed from sheared DNA that was end repaired and A-tailed using the NEBNext Ultra II DNA library prep kit for Illumina (New England Biolabs) before the ligation of dual-indexed TruSeq adapters and cleanup using 0.8X AMPure XP beads (Beckman-Coulter). Libraries were sequenced to an average depth of $\times 60$ on an Illumina HiSeqX system. Reads were aligned using BWA-MEM (version 0.7.6a).⁹ Structural variants were identified using Manta.¹⁰ Copy-number variants (CNVs) were identified with Control-FREEC.¹¹ Copy-number data were obtained for the discovery cohort using Affymetrix SNP6.0 arrays as previously described.^{1,12} All statistical tests were performed in R software (version 3.5.1). This study was reviewed and approved by the University of British Columbia-BC Cancer Research Ethics Board in accordance with the Declaration of Helsinki.

Results and discussion

FISH-cryptic rearrangements of *BCL2* and *MYC*

All FISH-detected *BCL2* and *MYC* rearrangements were detected by WGS structural variant calling, confirming the sensitivity of WGS to these events (Figure 1A; supplemental Table 1, available on the *Blood* Web site). Additional *BCL2* and *MYC* rearrangements were identified in the genomes of 3 cases each. Figure 1B describes 1 of 2 tumors in which the *BCL2* gene was inserted into the *IGH* locus, placing *BCL2* in close proximity to the ϵ_{μ} enhancer. The breakpoints in *IGH* and near the 3' untranslated region of *BCL2* were consistent with typical *BCL2-IGH* translocations.¹³ Importantly, the removal of *BCL2* from chromosome 18 left the regions targeted by breakapart FISH probes adjacent (supplemental Figure 1). In another case, 80 kb of the *IGK* locus, including the ϵ_k enhancer, was inserted telomeric to *BCL2* (Figure 1C). Two tumors harbored cryptic enhancer insertions near *MYC* (eg, 170 kb of the *ZCCHC7* locus including the *PAX5* super-enhancer inserted telomeric to *MYC*; Figure 1D). None of these enhancer insertions were large enough to separate the breakapart probes so as to be detectable by FISH (supplemental Figure 1).

Thus, 6 apparently non-HGBL-DH/TH tumors were confirmed to be HGBL-DH/TH through the use of WGS. All of the cases with cryptic *BCL2* or *MYC* rearrangements were positive for *BCL2* or *MYC* protein by immunohistochemistry, respectively (Figure 1A). Cryptic *MYC* translocations exclusively involved a nonimmunoglobulin partner, whereas *BCL2* rearrangements all involved immunoglobulin partner loci. In 2 tumors, the *MYC* locus was translocated adjacent to the *BCL6* superenhancer (supplemental Table 1), an event cryptic to both *MYC* and *BCL6* FISH. No other cryptic *BCL6* rearrangements were detected in this patient group. Considering these findings, breakapart FISH failed to detect a clinically significant proportion of HGBL-DH/THs, with cryptic HGBL-DH/TH-*BCL2* tumors representing 19% (6 of 31) of all HGBL-DH/TH-*BCL2* tumors in the original DHITsig discovery cohort.

CNVs enriched in DHITsig⁺ tumors

Although focal *MYC* gains were not exclusive to DHITsig⁺ tumors, several of the genomes had notable CNVs affecting *MYC* and/or pathways downstream of *MYC*, including 2 focal *MYC* gains and 1 case of double minute (Figure 2A). *MIR17HG* encodes the miR-17~92 microRNA cluster, which is a direct target of *MYC*.^{14,15} Copy gains affecting *MIR17HG* were identified in 6 of 20 DHITsig⁺ cases (Figure 2B) and may represent an avenue for dysregulation of *MYC* and its downstream targets in these cases.

A comparison of SNP array copy-number profiles from 179 GCB-DLBCLs, including the 20 cases described here, revealed that amplifications (copy number >3) of *MIR17HG* and *FCGR2B* and deletions of *CDKN2A* and 22q11.22 (*IGL*) were significantly enriched among DHITsig⁺ tumors (supplemental Figure 2). *FCGR2B* amplification is associated with rituximab resistance and may therefore contribute to treatment resistance among DHITsig⁺ tumors.^{12,16} Deletions of *CDKN2A* lead to decreased TP53 protein¹⁷ and represent an additional mechanism of TP53 inactivation in DHITsig⁺ tumors, along with the frequent *TP53* mutations described previously.³ The 22q11.22 deletion breakpoints observed by WGS were consistent with *IGL* VJ recombination.

A single genome harbored the 11q aberration pattern, which has been described among *MYC*⁻ BLs.¹⁸ The SNP array copy-number data identified 6 cases with the 11q aberration: 1 each in GCB DHITsig⁺ cases with or without genetic double hit, and 4 in GCB DHITsig⁻ tumors lacking *MYC* or *BCL2* rearrangements. Four 11q aberrations were confirmed by FISH (supplemental Figure 3). These results suggest that the 11q aberration is not associated with the DHITsig in DLBCL.

Among the genomes, there were 3 instances of focal promoter deletions of *PVT1*, including 1 in the double-minute chromosome (Figure 2C). The SNP array copy-number data did not identify any additional cases with this deletion. The *PVT1* long noncoding RNA gene contains intragenic enhancers that drive expression of *PVT1*, but in the absence of an active *PVT1* promoter they instead drive expression of *MYC*.¹⁹ Although the

number of occurrences limits our power to determine whether *PVT1* deletions are associated with DHITsig positivity, these results suggest that this is a rare, albeit recurrent, event that could promote *MYC* expression in DHITsig⁺ tumors.

In summary, genetic events affecting both *MYC* and *BCL2* were identified in 13 of 20 DHITsig⁺ tumors that were deemed non-HGBL-DH/THs by breakapart FISH. The identification of FISH-cryptic *MYC* and *BCL2* rearrangements in 6 cases highlights the limitation of FISH in identifying HGBL-DH/TH. The DHITsig phenotype can thus be attributed to a range of genetic events affecting *MYC*, *BCL2*, and downstream pathways, some of which are not revealed even by WGS, demonstrating that gene expression profiling is a more appropriate method to identify this biological group that constitutes high-risk GCB-DLBCL.

Acknowledgments

This research was supported by grants from the Terry Fox Research Institute (1061) and Canadian Institute for Health Research (R.D.M.) and MITACS Accelerate (R.D.M. and L.K.H.), a Scholar Award from the ASH Foundation (R.D.M.), and the BC Cancer Foundation. R.D.M. is a Michael Smith Foundation for Health Research Scholar.

Authorship

Contribution: L.K.H., B.M.G., J.T., M.A., C.K.R., A.J., and R.D.M. analyzed and interpreted the data; L.K.H. generated all figures; M.B., B.M., and S.B.-N. processed the tissues and performed FISH assays; and L.K.H., D.W.S., and R.D.M. conceived the study and wrote the manuscript.

Conflict-of-interest disclosure: A.J., D.W.S. and R.D.M. are named inventors on a patent application pertaining to the DHITsig. The remaining authors declare no competing financial interests.

ORCID profiles: L.K.H., 0000-0002-6413-6586; J.T., 0000-0002-5633-6123; S.B.-N., 0000-0002-2867-4037; M.A., 0000-0001-6945-0972; A.J., 0000-0002-6153-7595; B.M.G., 0000-0002-4621-1589; C.K.R., 0000-0001-6306-9361; R.D.M., 0000-0003-2932-7800.

Correspondence: Ryan D. Morin, Department of Molecular Biology and Biochemistry, Simon Fraser University, 8888 University Dr, Burnaby, BC, Canada; e-mail: rdmorin@sfu.ca; and David W. Scott, Department of Lymphoid Cancer Research, BC Cancer, 675 West 10th Ave, Vancouver, BC, Canada; e-mail: dscott8@bccancer.bc.ca.

Footnotes

Submitted 24 July 2019; accepted 8 September 2019. Prepublished online as *Blood* First Edition paper, 16 September 2019; DOI 10.1182/blood.2019002600.

*D.W.S. and R.D.M. contributed equally to this work.

Data will be deposited in EGA with accession number EGAS00001004285.

The online version of this article contains a data supplement.

The publication costs of this article were defrayed in part by page charge payment. Therefore, and solely to indicate this fact, this article is hereby marked "advertisement" in accordance with 18 USC section 1734.

REFERENCES

- Ennishi D, Mottok A, Ben-Neriah S, et al. Genetic profiling of *MYC* and *BCL2* in diffuse large B-cell lymphoma determines cell-of-origin-specific clinical impact. *Blood*. 2017;129(20):2760-2770.
- Scott DW, King RL, Staiger AM, et al. High-grade B-cell lymphoma with *MYC* and *BCL2* and/or *BCL6* rearrangements with diffuse large B-cell lymphoma morphology. *Blood*. 2018;131(18):2060-2064.
- Ennishi D, Jiang A, Boyle M, et al. Double-hit gene expression signature defines a distinct subgroup of germinal center B-cell-like diffuse large B-cell lymphoma. *J Clin Oncol*. 2019; 37(3):190-201.
- Copie-Bergman C, Cuillière-Dartigues P, Baia M, et al. *MYC*-IG rearrangements are negative predictors of survival in DLBCL patients treated with immunochemotherapy: a GELA/LYSA study. *Blood*. 2015;126(22):2466-2474.
- Sakr H, Cook JR. Identification of "double hit" lymphomas using updated WHO criteria: insights from routine *MYC* immunohistochemistry in 272 consecutive cases of aggressive B-cell lymphomas. *Appl Immunohistochem Mol Morphol*. 2019;27(6):410-415.
- King RL, McPhail ED, Meyer RG, et al. False-negative rates for *MYC* fluorescence *in situ* hybridization probes in B-cell neoplasms. *Haematologica*. 2019;104(6):e248-e251.
- Peterson JF, Pitel BA, Smoley SA, et al. Elucidating a false-negative *MYC* break-apart fluorescence *in situ* hybridization probe study by next-generation sequencing in a patient with high-grade B-cell lymphoma with *IGH/ MYC* and *IGH/BCL2* rearrangements. *Cold Spring Harb Mol Case Stud*. 2019;5(3): a004077.
- Wagener R, Bens S, Toprak UH, et al. Cryptic insertion of *MYC* exons 2 and 3 into the *IGH* locus detected by whole genome sequencing in a case of *MYC*-negative Burkitt lymphoma [published online ahead of print 9 May 2019]. *Haematologica*. doi: 10.3324/haematol.2018.208140.
- Li H. Aligning sequence reads, clone sequences and assembly contigs with BWA-MEM. <https://arxiv.org/abs/1303.3997>. Accessed 23 September 2019.
- Chen X, Schulz-Trieglaff O, Shaw R, et al. Manta: rapid detection of structural variants and indels for germline and cancer sequencing applications. *Bioinformatics*. 2016;32(8): 1220-1222.
- Boeva V, Popova T, Bleakley K, et al. Control-FREEC: a tool for assessing copy number and allelic content using next-generation sequencing data. *Bioinformatics*. 2012;28(3): 423-425.
- Arthur SE, Jiang A, Grande BM, et al. Genome-wide discovery of somatic regulatory variants in diffuse large B-cell lymphoma. *Nat Commun*. 2018;9(1):4001.
- Chong LC, Ben-Neriah S, Slack GW, et al. with DLBCL morphology. *Blood Adv*. 2018; 2(20):2755-2765.
- Benhamou D, Labi V, Getahun A, et al. The c-Myc/miR17-92/PTEN axis tunes PI3K activity to control expression of recombination activating genes in early B cell development. *Front Immunol*. 2018;9:2715.
- Mihailovich M, Bremang M, Spadotto V, et al. miR-17-92 fine-tunes *MYC* expression and function to ensure optimal B cell lymphoma growth. *Nat Commun*. 2015;6:8725.
- Lee CS, Ashton-Key M, Cogliatti S, et al. Expression of the inhibitory Fc gamma receptor IIB (FCGR2B, CD32B) on follicular lymphoma cells lowers the response rate to rituximab monotherapy (SAKK 35/98). *Br J Haematol*. 2015;168(1):145-148.
- Monti S, Chapuy B, Takeyama K, et al. Integrative analysis reveals an outcome-associated and targetable pattern of p53 and cell cycle deregulation in diffuse large B cell lymphoma. *Cancer Cell*. 2012;22(3):359-372.
- Salaverria I, Martin-Guerrero I, Wagener R, et al; Berlin-Frankfurt-Münster Non-Hodgkin Lymphoma Group. A recurrent 11q aberration pattern characterizes a subset of *MYC*-negative high-grade B-cell lymphomas resembling Burkitt lymphoma. *Blood*. 2014; 123(8):1187-1198.
- Cho SW, Xu J, Sun R, et al. Promoter of lncRNA gene PVT1 is a tumor-suppressor DNA boundary element. *Cell*. 2018;173(6): 1398-1412.e22.